

# CFD Analysis of Flow through Compressor Cascade

K.M.Pandey, S.Chakraborty, K.Deb

**Abstract**— This work aims at analyzing the flow behavior through a compressor cascade with the help of Computational Fluid Dynamics using the FLUENT software. An attempt has been made to study the effect of angle of attack or flow incidence angle on various flow parameters viz. static pressure, dynamic pressure, turbulence and their distribution in the flow field and predict the optimum range of angle of attack based on the above observations. Particularly, two principle parameters viz. the static pressure rise for the compressor cascade and the turbulence kinetic energy are considered in this analysis. It is observed that maintaining a slightly positive angle of flow incidence of +2 to +6 degrees is advantageous.

**Index Terms**—Cascade, CFD, Total Pressure, Temperature Magnitude, Viscosity, Thermal Conductivity

## I. INTRODUCTION

A fluid machine is a device which converts the energy stored by a fluid into mechanical energy or vice versa. The energy stored by a fluid mass appears in the form of potential, kinetic and intermolecular energy. The mechanical energy, on the other hand, is usually transmitted by a rotating shaft. In the development of the highly efficient modern axial flow compressor or turbine, the study of the two dimensional flow through a cascade of aerofoil has played an important role. An aerofoil is build up around a basic camber line, which is usually a circular or a parabolic arc. A camber line is thus the skeleton of the aerofoil. A thickness  $t$  is distributed over the camber line with the leading and trailing edge circles that finally form an aerofoil.

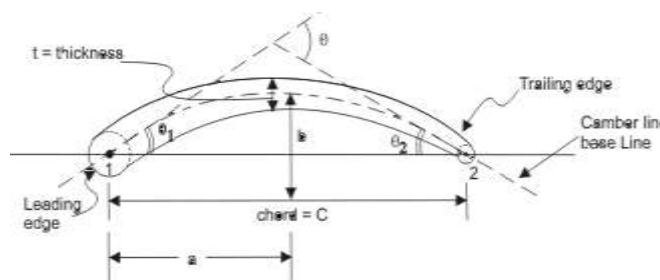


Figure 1: Cascade Nomenclature

In the above figure, the dotted line indicates the camber line and 'a' is the distance from the leading edge for maximum camber and 'b' is the maximum displacement from the chord line. Cascade geometry is defined completely by the aerofoil specification; pitch-chord ratio and the chosen setting i.e. stagger angle  $\lambda$  shown below.  $\Theta$  is called the aerofoil camber angle i.e.  $\Theta = \Theta_1 + \Theta_2$ . For a circular arc,  $\Theta_1 = \Theta_2 = \Theta/2$  and  $a/c = 0.5$ . For a parabolic arc  $a/c < 0.5$ .

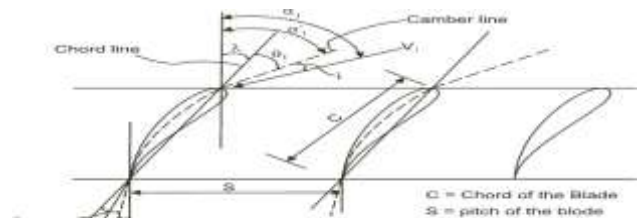


Figure 2: A compressor cascade-a

$\lambda$  = stagger angle (positive for a compressor cascade)

$\alpha_1' =$  blade inlet angle =  $\lambda + \Theta_1$

$\alpha_2' =$  blade outlet angle =  $\lambda - \Theta_2$

The angle of incidence 'i' is the angle made by the inlet flow  $V_1$  with the camber line. Under a perfect situation, the flow will leave along the camber line at the trailing edge of the blade. But it does not really happen so and there is a deviation which is denoted by ' $\delta$ '. Thus, the air inlet angle,  $\alpha_1 = \lambda + \Theta_1 + i$  Air outlet angle,  $\alpha_2 = \lambda - \Theta_2 - \delta$ . Hence,  $\epsilon =$  deflection of flow =  $\alpha_1 - \alpha_2 = \Theta + i - \delta$ . The blade efficiency or diffusion efficiency for a compressor cascade is defined as:

$\eta_b =$  (Actual rise in static pressure) / (Ideal static pressure rise)

$(\eta_b)_{comp\ cascade} = 1 - (2C_D) / (C_L \sin 2\alpha_m)$ , where  $C_D =$  Co-efficient of Drag and  $C_L =$  Co-efficient of Lift. It has been observed that the flow incidence angle has a huge effect on the flow behavior within the compressor cascade. In this work, an attempt has been made to determine the range of inlet flow angles which leads to the best performance of the compressor cascade.

## II. LITERATURE REVIEW

A tandem cascade was designed and it was analyzed by Qiushi, et al. [1]. According to their design model the front cascade adopts a supersonic profile to reduce the shock wave intensity turning the flow into subsonic, while the rear

Revised Manuscript Received on March 2012.

**Dr.K.M.Pandey**, Mechanical Engineering, National Institute of Technology, Silchar, Silchar, India, 9435173130, (e-mail: kmpandey2001@yahoo.com).

**S.Chakraborty**, Mechanical Engineering, NIT Silchar, Silchar, India, (e-mail: secondauthor@rediffmail.com).

**K.Deb**, Mechanical Engineering, National Institute of Technology, Silchar, Silchar, India, 8876723863, (e-mail: kamal.kd86@gmail.com).

cascade adopts a subsonic profile with a large camber offering the flow a large turning angle. They observed that the losses would be minimized if the leading edge of the rear cascade lies close to the pressure side of the front cascade at a distance of 20% pitch in pitch-wise direction without either axial spacing or overlapping in axial direction. Their 2D numerical test results show that, with the inflow mach no. of 1.25 and the turning angle of 52, the total pressure loss coefficient of the tandem cascade reaches 0.106, and the diffusion factor 0.745, and by adopting the finding and concerning the best relative position of the front to the rear cascade of tandem cascade, a high loaded fan stage with rotor tip speed of 495.32 m/s has successfully been developed. Bakhtar and So [2] studied the nucleating flow of steam in a cascade of supersonic blading by the time-marching method. This investigation follows the earlier experiment in which a case of 2D nucleating flow of steam in a cascade was investigated, but there were some numerical errors with the particular configuration. To discard the errors associated with the solution they assumed the bulk of the flow to be inviscid. They came to the conclusion that a finer mesh can be embedded into selected regions of the basic computational grid and its coordinates transformed if necessary. This increases the capability of the basic technique by increasing the accuracy in the selected region without an undue increase in the overall computing needs. Delery & Meauze [3] made an experimental analysis of the flow in a highly loaded fixed compressor cascade i.e. the ISO-cascade co-operative programme on code validation. Study was made in a two dimensional fixed geometry to reproduce the main physical features of the flow in a real compressor, including strong viscous flow. The objective of them was to show how a detailed qualification of the flow by different and complimentary method allows to establish a consistent physical picture of the flow in a cascade where 3D effects plays a dominant role. The experiments were carried out in the S5Ch transonic/supersonic wind tunnel. They found that the large expansion over the first part of the blade suction side is followed by a compression starting 30% downstream of the leading edge. They also found that, if kink, followed the start of the compression in the distribution indicative of the presence of a laminar separation bubble then at the blade mid portion, a rapid turning of the skin friction lines occurs and a zone of concentration of the visualization product forms. From their study it was possible to establish the flow topology which contains several complex and interacting vortical structures. Their results have been used to validate Navier–Stokes codes and different turbulence models. Another research work was done by Lio and Lin [4] on the slightly perturbed two-dimensional subsonic compressible potential flow through the cascade by direct boundary element methods(BEMs). They have performed their work in three BEM schemes: Scheme 1) Orthotropic medium method, Scheme 2) Equivalent cascade method, Scheme 3) Compressibility correction method. Using these three schemes, they have formulated a numerical calculation of the 2D subsonic compressible potential flow through a cascade, and used it to calculate the flow through the cascade

composed of seven identical K-7 compressor-blades. Their calculation results were compared with each other, and with the experimental results obtained on the same cascade in the range of angle of attack,  $i = -2.5^{\circ} - 10^{\circ}$ . It has been shown that these three direct BEM schemes lend themselves to calculation of the 2D slightly perturbed subsonic compressible potential flow through a cascade. Among them the orthotropic medium method is more natural and more trustworthy than the other two methods. State-of-the-art prediction of the aero-elastic stability of cascades in axial-flow turbo-machines is reviewed by another scholar named, Forsching [5]. He worked on the comprehensive formulation of the two- and three-dimensional classical (unstalled) flutter problem of tuned and mistuned rotor blade rows and bladed disc assemblies. Within the framework of linearized analysis, a complete and generalized theory in model form was presented, comprising the various formulations of the cascade flutter problem distributed in fragments throughout the literature. Brief outlines were also made of recent advances in unsteady aerodynamic methods for turbo-machinery aero-elastic applications. Secondly parametric study of the classical flutter stability characteristics of compressor and turbine cascades in subsonic and supersonic flow had been studied by them. Stability boundaries and dominant trends in flutter behavior are outlined, and the significant effects of blade mistuning on the aero-elastic stability of turbo-machine bladings were the main features of their study. Alawa, et al. [6] had shown how Rotor-blades' profile influence on a gas-turbine's compressor effectiveness. Their object of the work was to establish a relationship between changes in the incident rotor-blade angle due to compressor blade profile distortions and the required compressor power. This was achieved by measuring certain performance characteristics of an operational gas-turbine. The parameters relevant for the study at the inlet and outlet of the compressor, as well as the inlet and outlet of turbine were measured at the Ughelli Power Station, Delta State, Nigeria. Performance data were obtained from the pertinent daily log-sheets for the turbine. Design parameters were taken from the design manuals. Theoretical predictions from computer simulations had been compared with the corresponding measurements. They concluded that Compressor blade profile distortions can result in significant increases in the compressor power required per stage as well as the decreases in the gas turbine's isentropic efficiency. Compressor blade deteriorations and distortions lead to significant reduction in the gas-turbine's performance.

### III. METHODOLOGY

The 2D modelling scheme was adopted in GAMBIT and it was analysed using FLUENT. A compressor cascade model with zero degree flow angle of incidence was designed. The physical model is defined as follows:



Chord length	15 cm
Pitch-to-chord ratio (S/C)	0.52
Aspect ratio (H/C)	1.56
Outlet blade angle	4 degree
Stagger angle	22 degree
Number of blades	3
Operating Pressure	1 atm
Temperature	300 K
Velocity	20 m/s
Fluid	Air

The blade dimensions are taken from Ref. [7]. The model is shown below.

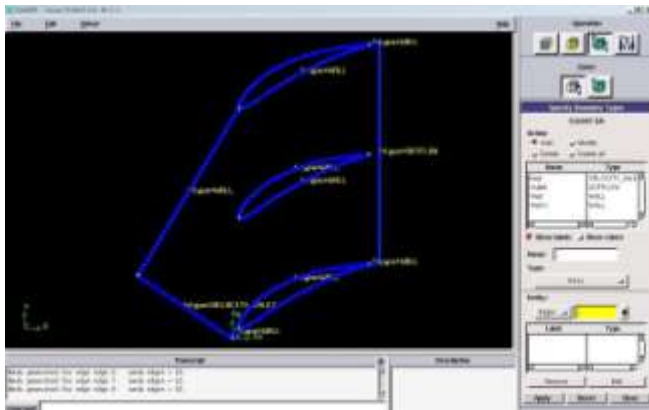


Figure 3: Compressor Cascade Model with boundary types.

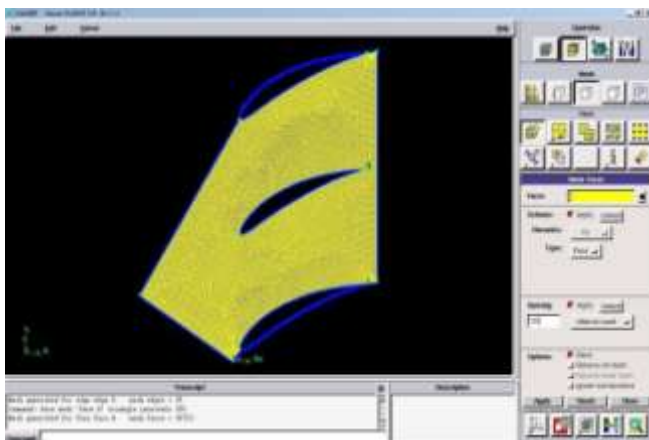


Figure 4: Compressor Cascade Model - Meshed.

The flow incidence angle is determined by the x and y velocity components which are as follows:

Table 1 : Velocity components for different flow incidence angles.

Flow Incidence Angle (a)(in degrees)	X Component of flow direction (cos a)	Y Component of flow direction (sin a)
-10	0.6691	0.7431
-6	0.6157	0.7880
-2	0.5592	0.8290
0	0.5299	0.8481
2	0.5	0.8660
6	0.4384	0.8988
10	0.3746	0.9272

The grid independence test is done which involves transforming the generated physical model into a mesh with number of node points depending on the fineness of the mesh. The various flow properties were evaluated at these node points. The extent of accuracy of result depended to a great extent on the fact that how fine the physical domain was meshed. After a particular refining limit the results changes no more. At this point it is said that grid independence is achieved. The results obtained for this mesh is considered to be the best. This mesh formation was done with GAMBIT.

#### IV. RESULTS AND ANALYSIS

The various contours of the flow parameters such as pressure, turbulence, velocity etc in the flow field for the different models are given below. The red colored regions are the regions where the properties attain their maximum values. The blue colored regions indicate the regions where the properties are at their minimum. The properties that were analyzed for the various models are-

1. Static Pressure
2. Dynamic Pressure
3. Total Pressure
4. Velocity Magnitude
5. Velocity Angle
6. Turbulence Kinetic Energy
7. Effective Viscosity
8. Effective thermal Conductivity

A. Flow incidence angle:-10 degree (a=angle of attack)

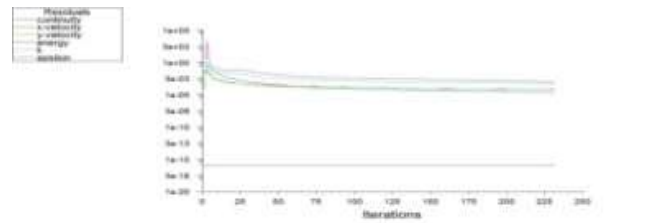


Figure 5: Plot of Scaled Residuals (a = -10 degrees)



Figure 6: Contour of Static Pressure (a = -10 degrees)

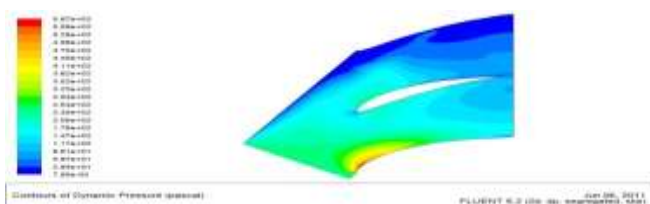


Figure 7: Contour of Dynamic Pressure (a = -10 degrees)

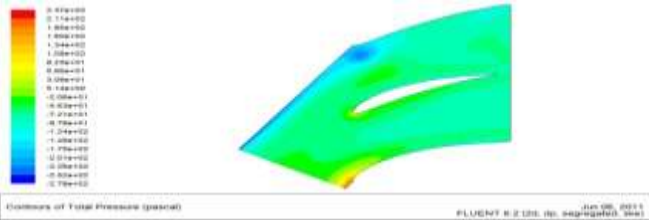


Figure 8: Contour of Total Pressure (a = -10 degrees)

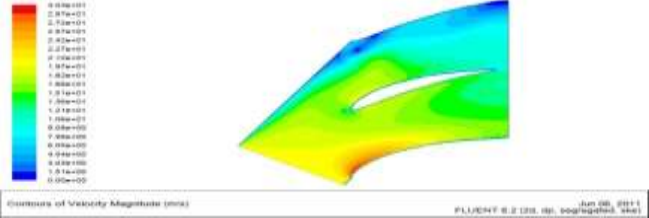


Figure 9: Contour of Velocity Magnitude (a = -10 degrees)

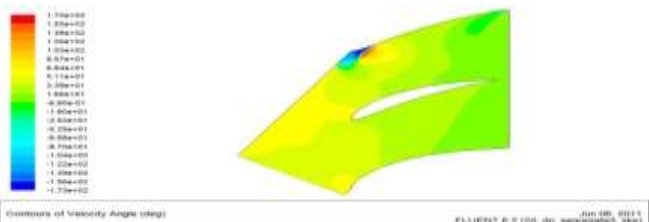


Figure 10: Contour of Velocity Angle (a = -10 degrees)

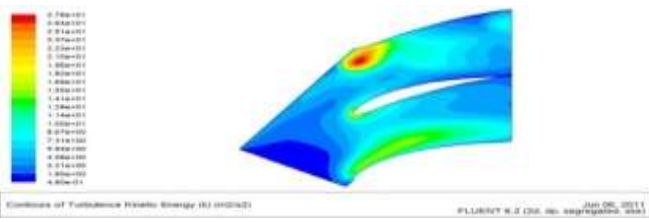


Figure 11: Contour of Turbulence Kinetic Energy (a = -10 degrees)

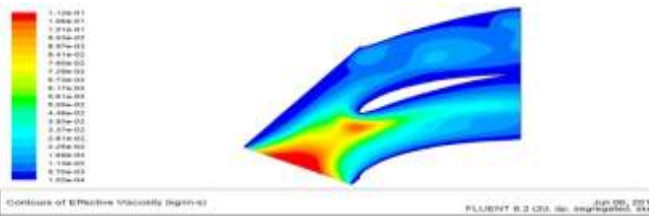


Figure 12: Contour of Effective Viscosity (a = -10 degrees)

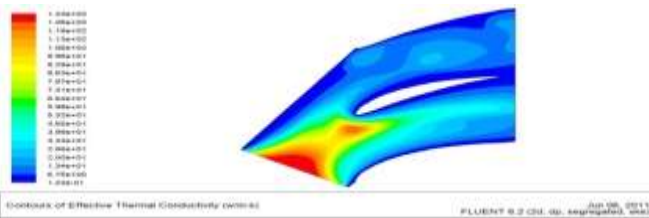


Figure 13: Contour of Effective Thermal Conductivity (a = -10 degrees)

B. Flow incidence angle: -6 degrees

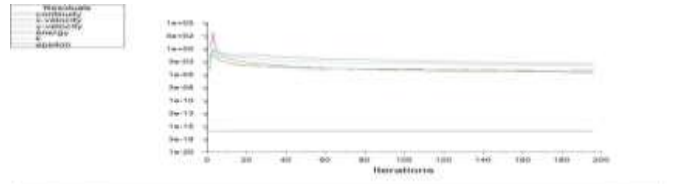


Figure 14: Plot of Scaled Residuals (a = -6 degrees)

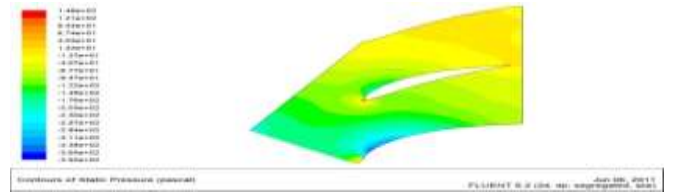


Figure 15: Contour of Static Pressure (a = -6 degrees)

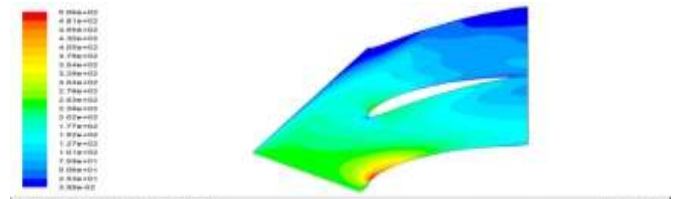


Figure 16: Contour of Dynamic Pressure (a = -6 degrees)

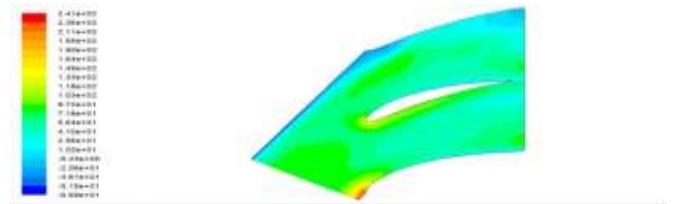


Figure 17: Contour of Total Pressure (a = -6 degrees)

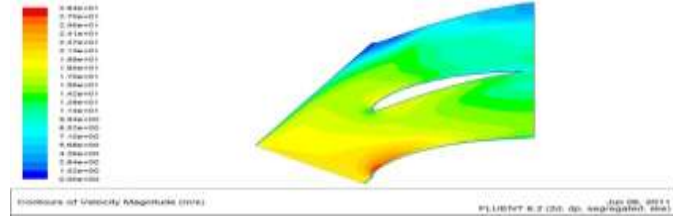


Figure 18: Contour of Velocity Magnitude (a = -6 degrees)

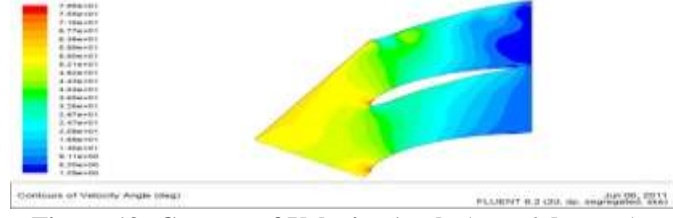


Figure 19: Contour of Velocity Angle (a = -6 degrees)

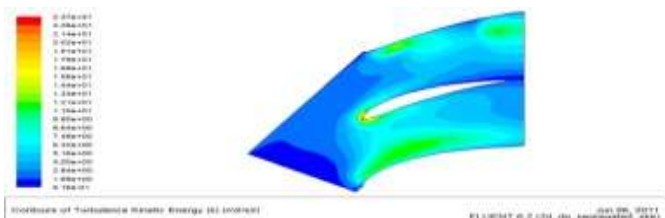


Figure 20: Contour of Turbulence Kinetic Energy ( $\alpha = -6$  degrees)

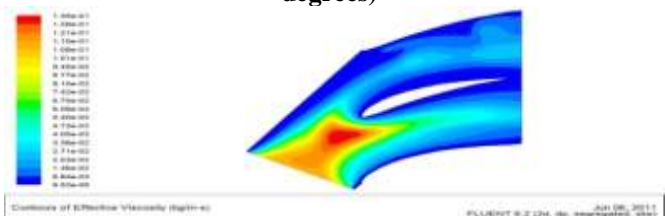


Figure 21: Contour of Effective Viscosity ( $\alpha = -6$  degrees)

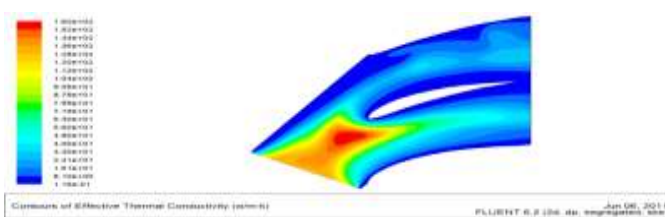


Figure 22: Contour of Effective Thermal Conductivity ( $\alpha = -6$  deg.)

C. Flow incidence angle: -2 degrees

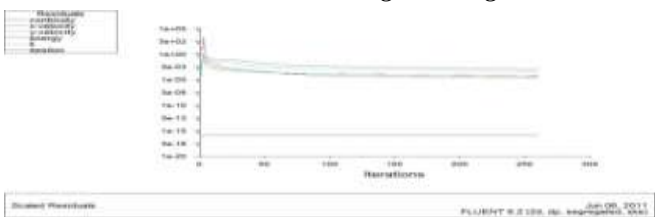


Figure 23: Plot of Scaled Residuals ( $\alpha = -2$  degrees)

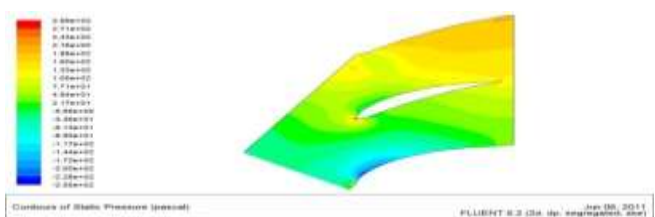


Figure 24: Contour of Static Pressure ( $\alpha = -2$  degrees)

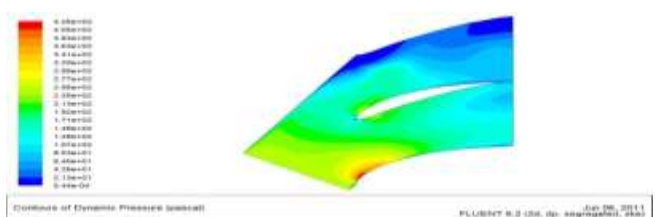


Figure 25: Contour of Dynamic Pressure ( $\alpha = -2$  degrees)

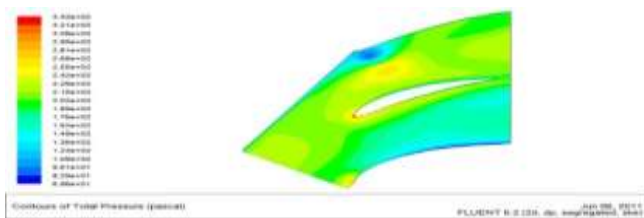


Figure 26: Contour of Total Pressure ( $\alpha = -2$  degrees)

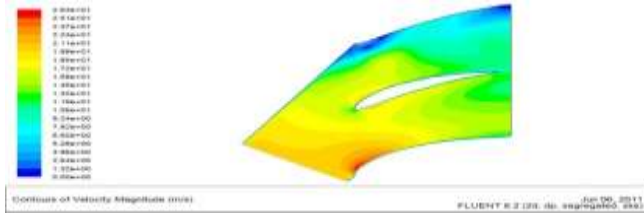


Figure 27: Contour of Velocity Magnitude ( $\alpha = -2$  degrees)



Figure 28: Contour of Velocity Angle ( $\alpha = -2$  degrees)

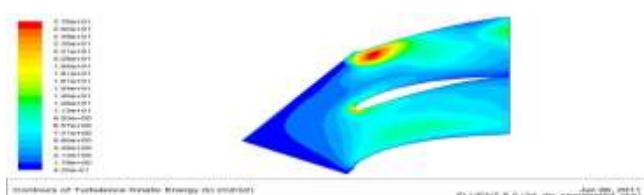


Figure 29: Contour of Turbulence Kinetic Energy ( $\alpha = -2$  degrees)

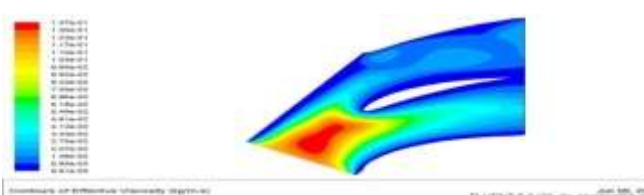


Figure 30: Contour of Effective Viscosity ( $\alpha = -2$  degrees)

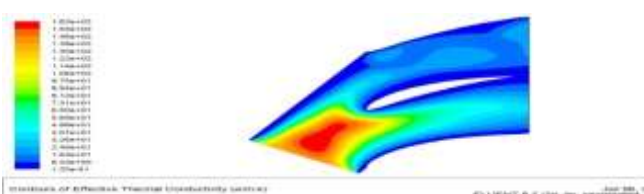


Figure 31: Contour of Effective Thermal Conductivity ( $\alpha = -2$  deg.)

D. Flow incidence angle: 0 degree

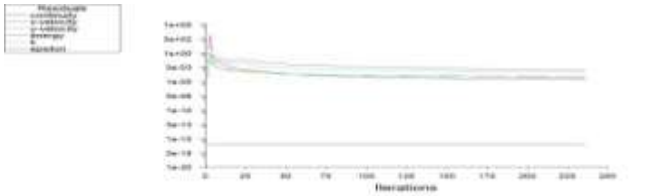


Figure 32: Plot of Scaled Residuals ( $\alpha = 0$  degree)

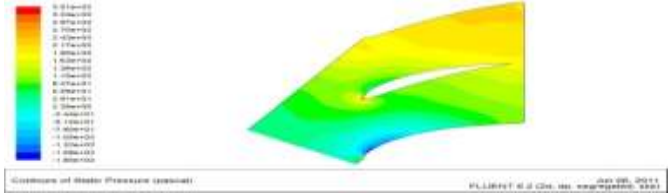


Figure 33: Contour of Static Pressure ( $\alpha = 0$  degree)

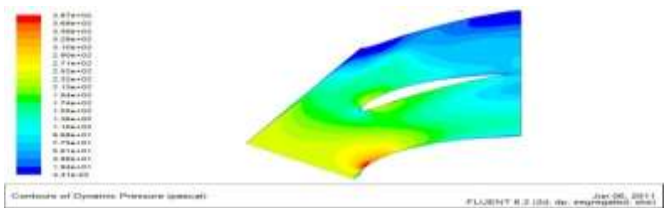


Figure 34: Contour of Dynamic Pressure ( $\alpha = 0$  degree)

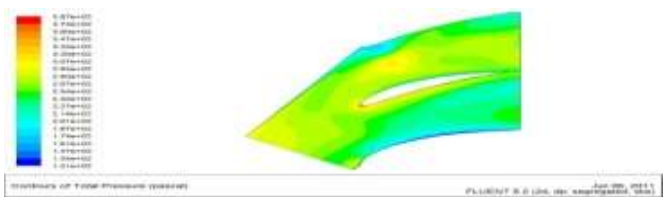


Figure 35: Contour of Total Pressure ( $\alpha = 0$  degree)

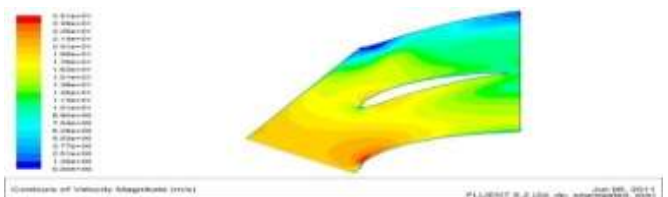


Figure 36: Contour of Velocity Magnitude ( $\alpha = 0$  degree)



Figure 37: Contour of Velocity Angle ( $\alpha = 0$  degree)

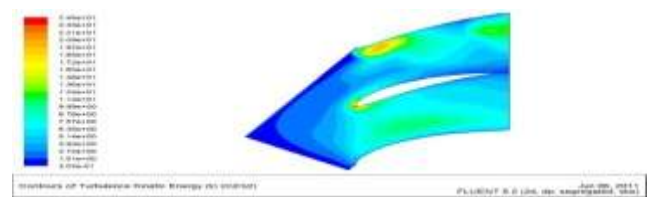


Figure 38: Contour of Turbulence Kinetic Energy ( $\alpha = 0$  degree)

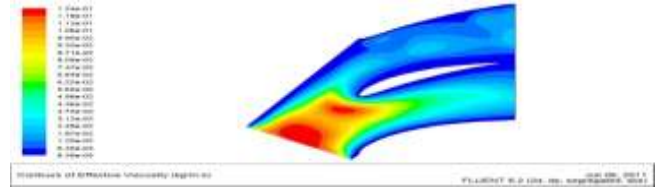


Figure 39: Contour of Effective Viscosity ( $\alpha = 0$  degree)

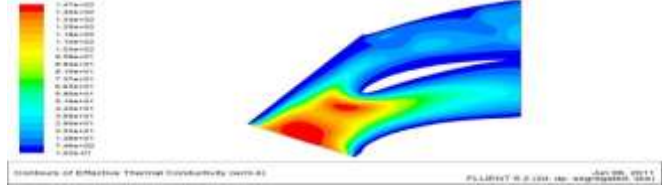


Figure 40: Contour of Effective Thermal Conductivity ( $\alpha = 0$  degree)

E. Flow incidence angle: +2 degree

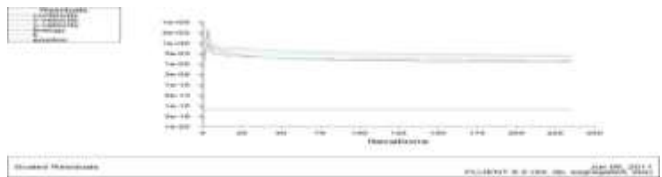


Figure 41: Plot of Scaled Residuals ( $\alpha = +2$  degrees)

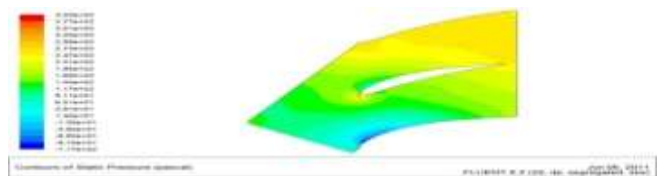


Figure 42: Contour of Static Pressure ( $\alpha = +2$  degrees)

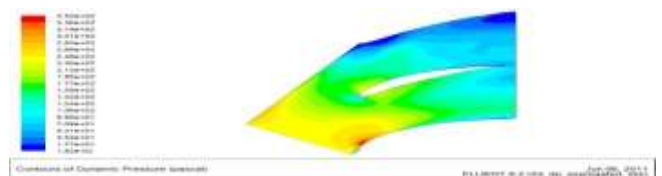


Figure 43: Contour of Dynamic Pressure ( $\alpha = +2$  degrees)

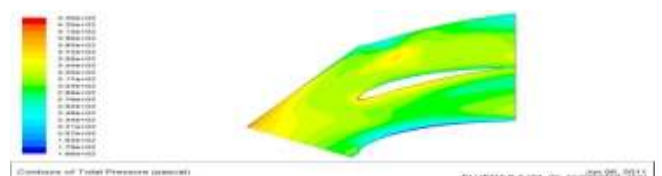


Figure 44: Contour of Total Pressure ( $\alpha = +2$  degrees)

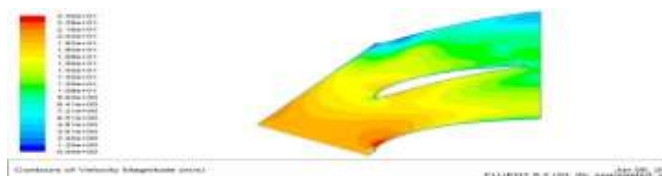


Figure 45: Contour of Velocity Magnitude ( $\alpha = +2$  degrees)

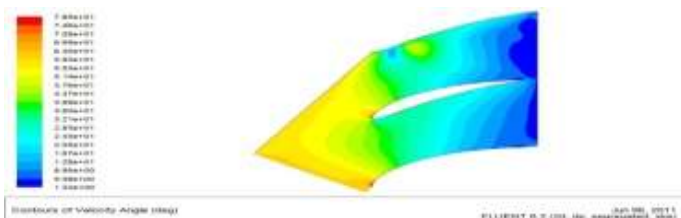


Figure 46: Contour of Velocity Angle ( $\alpha = +2$  degrees)

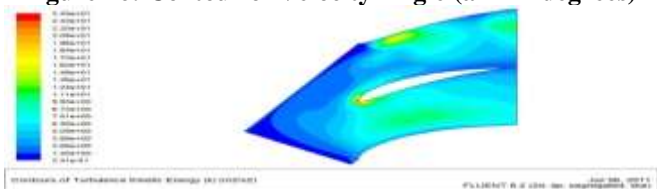


Figure 47: Contour of Turbulence Kinetic Energy ( $\alpha = +2$  degrees)

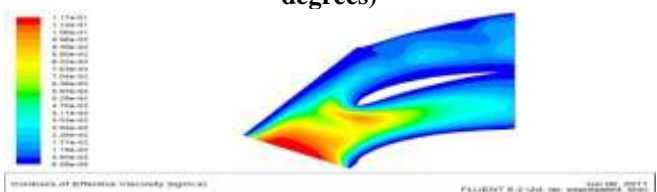


Figure 48: Contour of Effective Viscosity ( $\alpha = +2$  degrees)

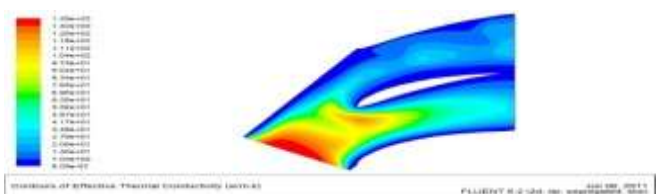


Figure 49: Contour of Effective Thermal Conductivity ( $\alpha = +2$  deg.)

F. Flow incidence angle: +6 degree

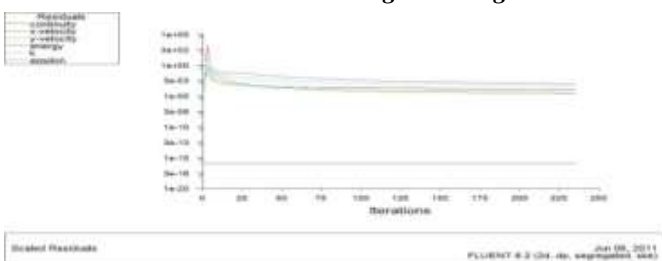


Figure 50: Plot of Scaled Residuals ( $\alpha = +6$  degrees)

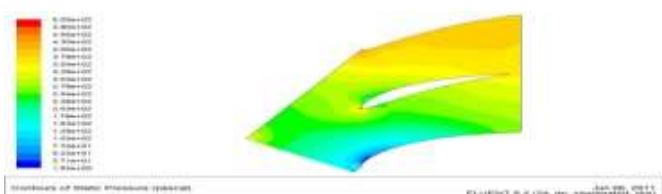


Figure 51: Contour of Static Pressure ( $\alpha = +6$  degrees)

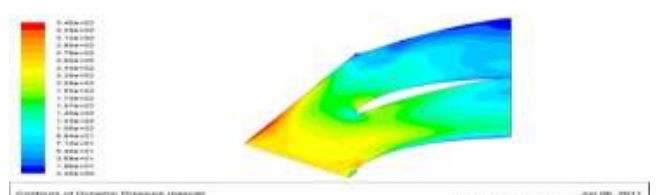


Figure 52: Contour of Dynamic Pressure ( $\alpha = +6$  degrees)

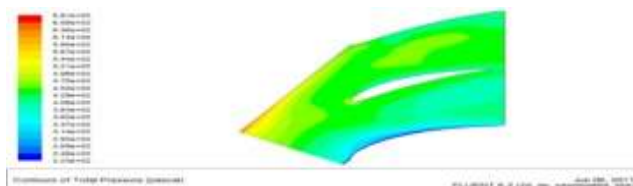


Figure 53: Contour of Total Pressure ( $\alpha = +6$  degrees)

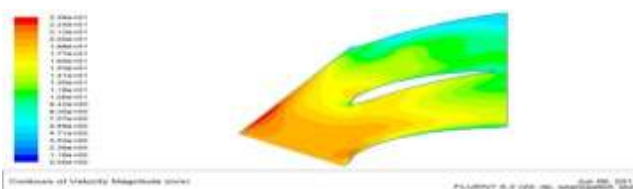


Figure 54: Contour of Velocity Magnitude ( $\alpha = +6$  degrees)

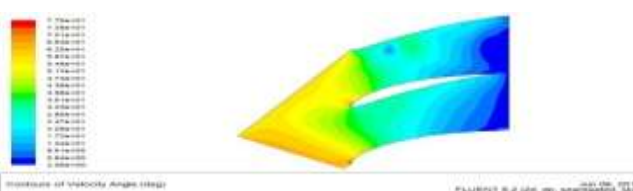


Figure 55: Contour of Velocity Angle ( $\alpha = +6$  degrees)

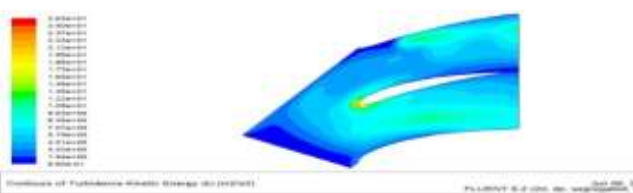


Figure 56: Contour of Turbulence Kinetic Energy ( $\alpha = +6$  degrees)



Figure 57: Contour of Effective Viscosity ( $\alpha = +6$  degrees)

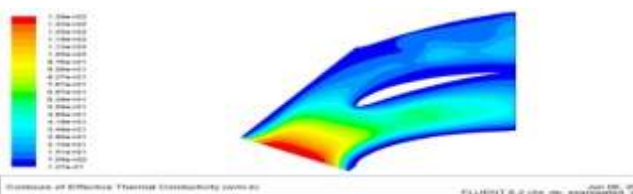


Figure 58: Contour of Effective Thermal Conductivity ( $\alpha = +6$  deg.)

G. Flow incidence angle: +10 degree

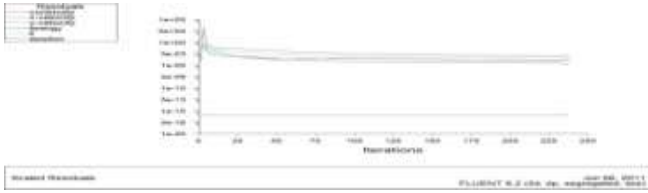


Figure 59: Plot of Scaled Residuals (a = +10 degrees)

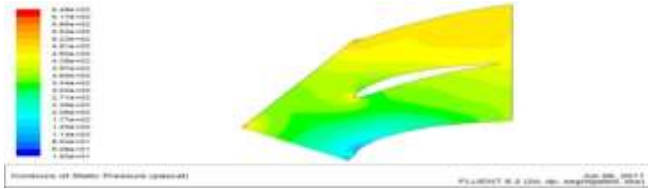


Figure 60: Contour of Static Pressure (a = +10 degrees)

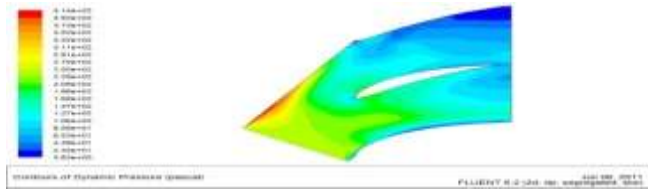


Figure 61: Contour of Dynamic Pressure (a = +10 degrees)

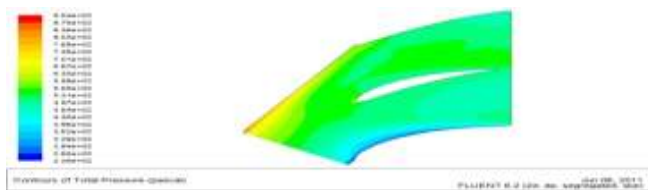


Figure 62: Contour of Total Pressure (a = +10 degrees)

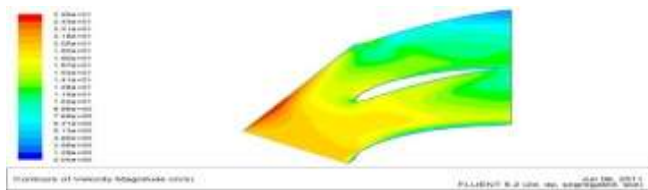


Figure 63: Contour of Velocity Magnitude (a = +10 degrees)

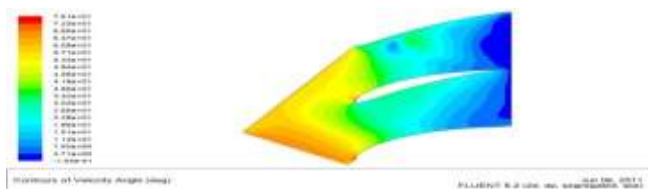


Figure 64: Contour of Velocity Angle (a = +10 degrees)

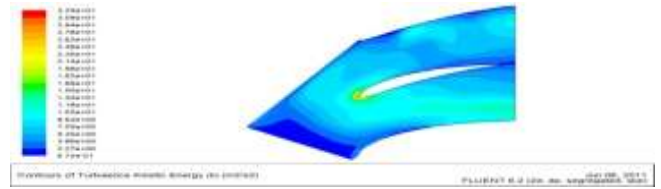


Figure 65: Contour of Turbulence Kinetic Energy (a = +10 degrees)

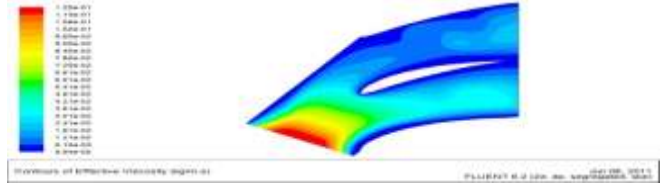


Figure 66: Contour of Effective Viscosity (a = +10 degrees)

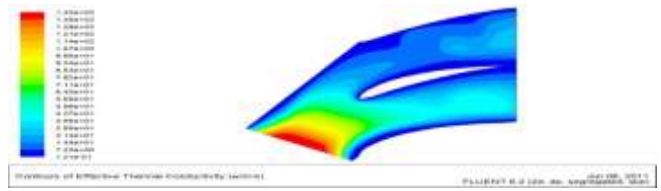


Figure 67: Contour of Effective Thermal Conductivity (a = +10 degrees)

V. CONCLUSION

It is observed from these contours that the static pressure for a compressor cascade increases along the cascade flow field, while the dynamic pressure and velocity decreases. The total pressure shows a layer-by-layer pattern over the blade profile. The velocity angle at any point in the flow field indicates the direction in which the flow is flowing at that point. The turbulence kinetic energy shows a decreasing value from the inlet. It can be noted that the effective viscosity and effective thermal conductivity is higher at regions of higher turbulence. This can be attributed to the fact that due to turbulence, a greater inter-mixing of the fluid molecules occur leading to increased resistance to flow, increasing the heat conductivity at the same time. A comparison of the contours of static pressure for the different inlet flow angles gives the following values:

Table 2: Static Pressure rise for different flow incidence angles.

Flow Incidence Angle (in degree)	Static Pressure Rise (bar)
-10	121.223
-6	123.247
-2	141.156
0	141.552
2	142.39
6	137.327
10	127.948

Plotting these values, a bell shaped curve is obtained which show its peak value at around +2 degrees. This is shown below.

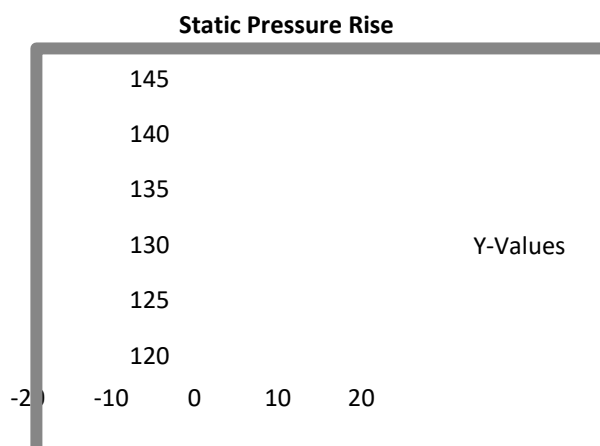


**Figure 68: Plot of Static Pressure Rise (in bar) v/s Flow Incidence Angle (in degrees)**

Greater the pressure rise, more is the work done by the compressor cascade with the same input parameters. A comparison of the Turbulence Kinetic Energy shows the following:

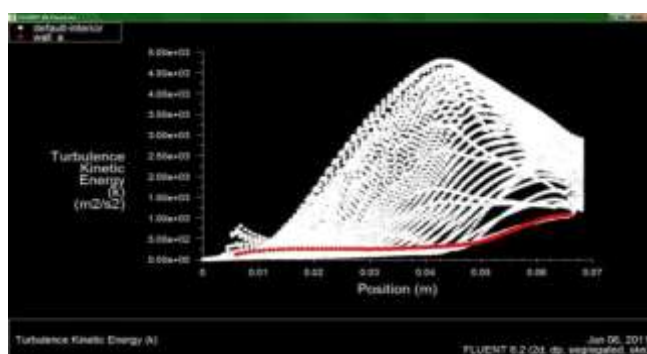
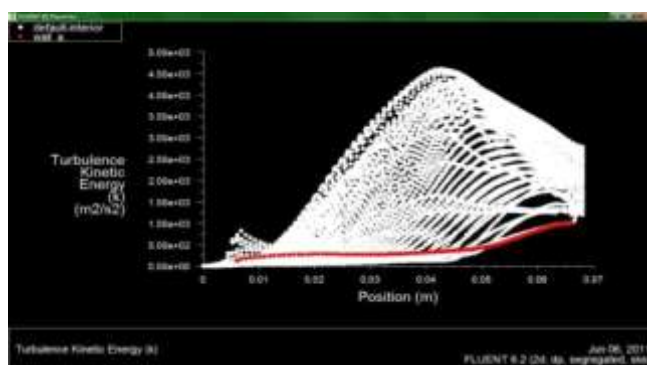
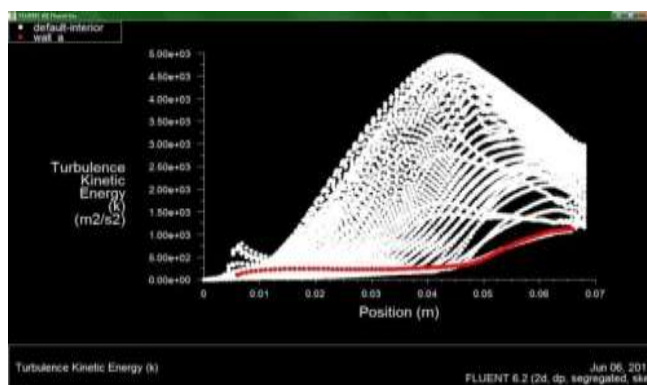
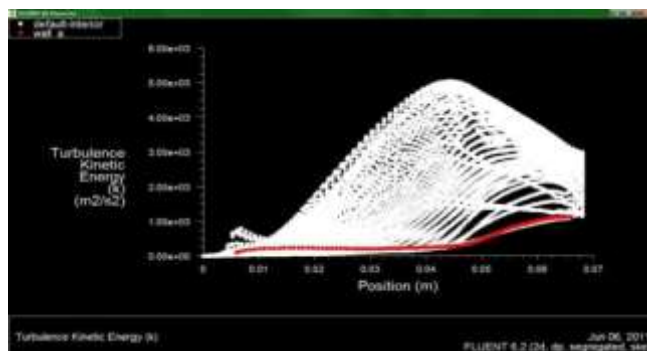
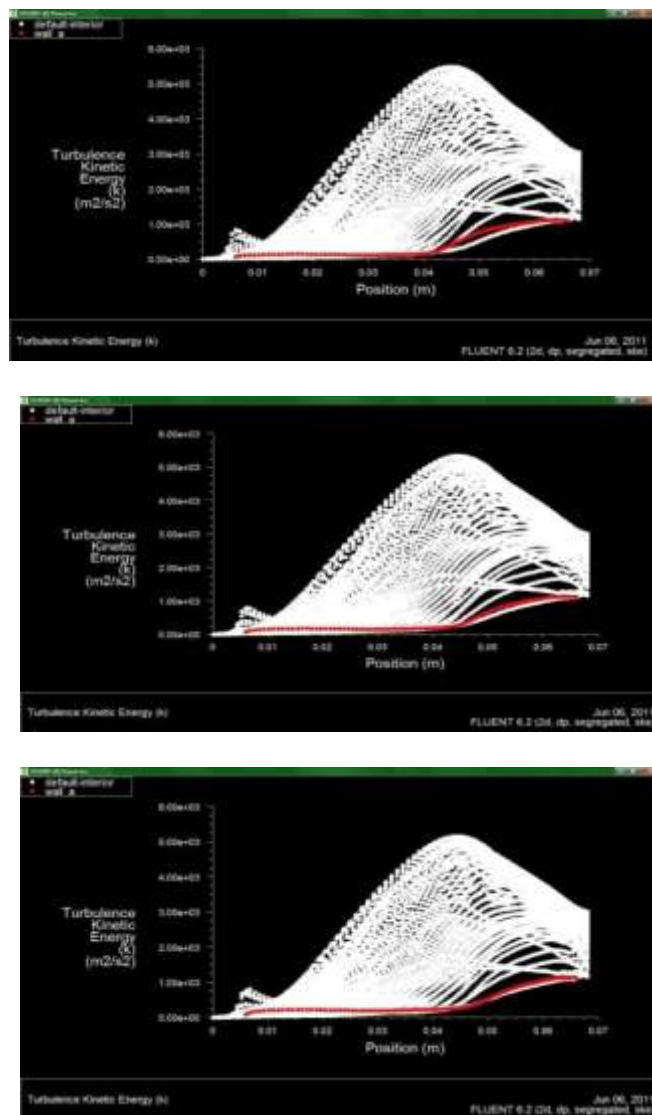


**Figure 69: Comparison of Turbulence Kinetic Energy for Compressor Cascade in sequence of -10, -6, -2, 0, +2, +4, +6 and +10.**

It can be noticed that the Turbulence Kinetic Energy shows a gradual decrease towards positive angles of attack, particularly in the range of +2 to +6 degrees. Thus maintaining a positive flow incidence angle in the range of +2 to +6 degrees would be advantageous.

## VI. SCOPE FOR FUTURE WORK

The analysis done on the cascade models falls short of a more realistic evaluation of flow parameters due to the absence of the stator as applicable in turbo-machines. Due to this, the inlet flow conditions more or less deviates from the actual ones. Also, a three dimensional model of the cascade will be able to simulate the flow conditions in a more effective and realistic manner. The computational results should be validated by experimental work performed under controlled conditions.

Hence future work in this direction, which includes a complete stage, involving a stator and a rotor, designed in the three dimensions, can provide a better ground for analyzing the flow through a cascade followed by experimental work to validate the computational results.

## ACKNOWLEDGEMENT

The authors acknowledge the financial help provided by AICTE from the project AICTE: 8023/RID/BOIII/NCP(21) 2007-2008 .The Project id at IIT Guwahati is ME/P/USD/4.

## REFERENCES

1. Li Qiushi, Wu Hong, and Zhou Sheng, "Application Of Tandem Cascade To Design Of Fan With Supersonic Flow", Chinese Journal of Aeronautics, Elsevier; 23(2010):9-14
2. F.Bakhtar and K.S So, "A Study Of Nucleating Flow Of Steam In A Cascade Of Supersonic Blading By The Time-Marching Method", International Journal Of Heat & Fluid Flow, Vol. 12, No.1,Butterworth-Heinemann,1991.
3. J. Delery & G. Meauze, "A Detailed Experimental Analysis Of The Flow In A Highly Loaded Fixed Compressor Cascade: The Iso-Cascade Co-Operative Programme On Code Validation", Aerospace Science & Technology 7,Elsevier;2009:1-9.
4. A.X. Lio and C.X. Lin, "Three BEM Schemes For The Calculating Of Subsonic Compressible Plane Cascade Flow", Engineering Analysis with Boundary Elements 11; 1993 : 25-32.
5. H. Forsching, "Aero-elastic stability of Cascades in Turbo-Machinery", Prog. Aerospace Science, Vol. 30 Pergamon;1994: 213-216.
6. B.T. Lebele Alawa, H.I. Hart, S.O.T. Ogaji, S.D. Probert, "Rotor Blades' Profile Influence On A Gas Turbine's Compressor Effectiveness", Applied Energy 85 , Elsevier; 2008, 494-505.
7. U. K. Saha, B. Roy, "Experimental Investigations on Tandem Compressor Cascade Performance at Low Speeds", Experimental Thermal and Fluid Science, Elsevier; 1997; 14:263-276.

## AUTHOR PROFILE



**Dr. K.M.Pandey** did his B.Tech in 1980 from BHUIT Varanasi, India in 1980.He obtained M.Tech. in heat power in 1987 .He received PhD in Mechanical Engineering in 1994 from IIT Kanpur. He has published and presented more than 200 papers in International & National Conferences and Journals. Currently he is working as Professor of the Mechanical .Engineering Department, National Institute of Technology, Silchar,Assam, India..He also served the department in the capacity of head from July 07 to 13 July 2010. He has also worked as faculty consultant in Colombo Plan Staff College, Manila, Philippines as seconded faculty from Government of India. His research interest areas are the following: Combustion, High Speed Flows,Technical Education, Fuzzy Logic and Neural Networks , Heat Transfer, Internal Combustion Engines, Human Resource Management, Gas Dynamics and Numerical Simulations in CFD area from Commercial Software's. Currently he is also working as Dean, Faculty Welfare at NIT Silchar, Assam, India.  
Email:kmpandey2001@yahoo.com.

**S.Chakraborty** has completed his B.Tech from NIT Silchar in 2011.



**K.Deb** is currently doing his M.Tech from NIT Silchar, he also qualified GATE in 2011,his research interests are CFD, Combustion and Gasification.

